Role of Polar and Enthalpic Effects in the Addition of Methyl Radical to Substituted Alkenes: A Density Functional Study Including Solvent Effects

Roger Arnaud,*[,1a] Nicolas Bugaud,[1a] Valentina Vetere,[1b] and Vincenzo Barone*[,1b]

Contribution from the Laboratoire d'Etudes Dynamiques et Structurales de la Sélectivité (LEDSS), UMR CNRS 5616, Université Joseph Fourier, 301 Avenue de la Chimie, BP 53X, F-38041 Grenoble, France, and Dipartimento di Chimica, Università Federico II, via Mezzocanone 4, I-80134, Napoli, Italy

Received November 13, 1997. Revised Manuscript Received March 26, 1998

Abstract: The addition of methyl radical to mono- and disubstituted alkenes has been studied by a hybrid Hartree−Fock/density functional method taking into account solvent effects by the polarizable continuum model. The reliability of the electronic approach has been verified by comparison with refined post-Hartree−Fock computations and with experimental data. Environmental effects do not alter the trends of in vacuo computations due to the low dielectric constant of the solvent and to the lack of significant charge separation effects. Use of substrates characterized by captodative effects and comparison with a genuine nucleophilic radical (CH_2OH) allow one to unequivocally conclude that CH_3 does not behave as a nucleophile. As a consequence polar effects are negligible and activation barriers are governed by the stability of the forming radical. These trends are confirmed by electron population analysis and evaluation of charge-transfer energies.

1. Introduction

The addition of free radicals to molecules containing unsaturated bonds is well recognized as one of the most powerful bond-forming reactions and represents the central step in many polymerization processes;[2,3] furthermore, it plays an important role in a number of biological mechanisms.[4,5] These reactions are generally strongly exothermic, since a σ bond is formed and a π bond is broken. However, the rate constants vary strongly with radical and alkene substitution. According to extensive mechanistic studies, polar, steric, and enthalpic effects all play a role in determining reactivity.[2,3,6,7] Additions to mono- ($H_2C{=}CHX$) and di- ($H_2C{=}CXY$) substituted alkenes invariably occur at the unsubstituted carbon atom. Under such circumstances steric effects (exerted only by β-substituents) are negligible, but the relative role of polar and enthalpic factors for the addition of methyl radical is still controversial. On the basis of a correlation between rate constants and electronic affinities of the alkenes, Fischer and co-workers[7] came to the conclusion that polar contributions play a significant role in such reactions. On the other hand, refined quantum mechanical computations for some of the simplest systems[8] suggest that the main effect governing activation barriers in the addition of CH_3 to monosubstituted alkenes is the reaction enthalpy. Further insight into this problem can be obtained, in our opinion, by a systematic quantum mechanical approach provided that the computational model couples the reliability of the results with a sufficient rapidity to deal with a significant number of systems even of quite large dimensions. This is even more important taking into account that non potential energy effects (especially entropy) should be carefully investigated due to some simplifying assumptions made in the analysis of experimental results.[7] Furthermore, the role of solvent has been completely neglected in previous theoretical investigations.

While the Hartree−Fock (HF) method can possibly provide reasonable structures for the stationary points (minima and transition states) governing radical additions, only the most sophisticated post-HF models provide sufficiently accurate reaction barriers.[9] Unfortunately, this class of methods is too expensive for systematic studies of large systems. In the last few years, much interest has been devoted to methods rooted into the density functional theory (DFT)[10] which are at the heart of a convenient computational approach capable of describing successfully problems previously covered exclusively by post-HF methods. In particular, hybrid HF/DFT methods[11] are extremely promising for the study of structures, spectroscopic properties, and reactivity of free radicals.[12−15] Although these

(1) (a) Université Joseph Fourier. (b) Università Federico II.
(2) Tedder, J. M. *Angew. Chem., Int. Ed. Engl.* **1982**, *21*, 401.
(3) Giese, B. *Angew. Chem., Int. Ed. Engl*. **1983**, *22*, 753.
(4) Von Sonntag, C. *The Chemical Basis of Radiation Biology*; Taylor & Francis: London, 1987; Chapter 6.
(5) Hoganson, W.; Babcock, G. T. *Biochemistry* **1992**, *31*, 11874.
(6) Heberger, K.; Fischer, H. *Int. J. Chem. Kinet*. **1993**, *113*, 4324.
(7) (a) Zytowski, T.; Fischer, H. *J. Am. Chem. Soc*. **1996**, *118*, 437. (b) Fischer, H. In *Free Radicals in Biology and Environment*, Minisci, F., Ed.; Kluwer: Dordrecht, 1997; p 69. (c) Zytowski, T.; Fischer, H. *J. Am. Chem. Soc*. **1997**, *119*, 12869.
(8) (a) Wong, M. W.; Pross, A.; Radom, L. *J. Am. Chem. Soc*. **1993**, *115*, 11050. (b) *Ibid*. **1994**, *116*, 6284.
(9) For an assessment of ab initio procedures, see: (a) Wong, M. W.; Radom, L. *J. Phys. Chem*. **1995**, *99*, 8582. (b) Heuts, J. P. A.; Gilbert, R. G.; Radom, L. *J. Phys. Chem*. **1996**, *100*, 18997.
(10) Parr, R. G.; Yang, W. *Density-Functional Theory of Atoms and Molecules*; Oxford University Press: New York, 1989.
(11) Becke, A. D. *J. Chem. Phys.* **1993**, *98*, 1372.
(12) Barone, V.; Adamo, C. *Chem. Phys. Lett*. **1994**, *224*, 432; erratum **1994**, *228*, 499.
(13) Barone, V. *J. Chem. Phys*. **1994**, *101*, 10666.
(14) Barone, V. In *Advances in Density Functional Methods, part I*; Chong, D. P., Ed.; World Scientific Publishing Co.: Singapore, 1995; Chapter 8, p 278.
(15) Baker, J.; Muir, M.; Andzelm. *J. Chem. Phys*. **1995**, *102*, 2063.

S0002-7863(97)03896-1 CCC: $15.00
Published on Web 05/29/1998

models have been recently applied to simple radical addition reactions,[16] to the best of our knowledge, no systematic study on the role of substituents in modifying radical reactivity has been performed till now.

Furthermore, one of us has recently implemented[17,18] a very effective continuum solvent model (the polarizable continuum model, PCM[19]) in the Gaussian series of programs,[20] and a number of tests have shown that reliable thermodynamic, kinetic, and spectroscopic parameters can be obtained for radical species by the combined use of PCM and DFT computational methods.[21,22] Here we apply this protocol to the energetics of CH_3 addition to 15 mono- and disubstituted alkenes for most of which reliable experimental data have been recently published.[7] Furthermore, some of these systems have been previously investigated by a refined post-HF approach,[8] thus allowing a further validation of our computational approach. Our study attempts to answer the following questions: (1) How do hybrid HF/DFT methods perform compared to high-level post-HF approaches? (2) How reliable are they in reproducing energetic features compared to experiment? (3) To what extent do solvent effects modify activation and reaction enthalpies evaluated in vacuo? (4) What is the role of thermodynamic and polar contributions in determining the rate of methyl additions?

Concerning the last point, we recall that, when polar contributions dominate, nucleophilic radicals react preferentially with electron-deficient alkanes and the reaction rate shows a good correlation with the electron affinity (EA) of the olefin. In the same vein, electrophilic radicals prefer electron-rich substrates and the reaction rate is related to the ionization potential (IP) of the alkene. On the other hand, a good correlation between reaction rates and reaction enthalpies (ΔH_r) is diagnostic of a dominant role of the strength of the forming bond (usually referred to as the enthalpic effect).[7a,8] In the case of methyl radical, the correlation between rates and IPs is definitely poor,[7] but the situation is more involved concerning EAs and ΔH_r values due to a significant direct correlation between these two quantities. However, if the geminal substituents of an alkene are an electron donor (D) and an electron acceptor (A) group, respectively, the product is stabilized by the so-called captodative effect.[23] In this case, the strong enhancement of the reaction exothermicity is not accompanied by an increase of the electronic affinity of $CH_2{=}CDA$. Thus, a significant increase of the reaction rate should point out a dominant role of enthalpic effects. In the present study, we have considered two simple alkenes with geminal D and A substituents ($H_2C{=}C(NH_2)CN$ and $H_2C{=}C(NH_2)CHO$). Although experimental data are not available for these systems, the very good correlation between experimental and B3LYP values for the other substituted alkenes (vide infra) make us quite confident in the use of B3LYP activation energies for correlation purposes. It would be, however, interesting to have experimental data for this kind of substrate.

2. Computational Methods

All the computations are based on the unrestricted Kohn−Sham (UKS) approach to DF theory[10] as implemented in the Gaussian 94 package.[20] On the grounds of previous experience,[13−16] we have selected the so-called B3LYP hybrid functional, which combines HF and Becke[24] exchange terms with the Lee−Yang−Parr correlation functional,[25] in the same ratios as those optimized by Becke for a similar (although not identical) functional.[26] The prototypical addition of CH_3 to ethylene has been studied by several standard basis sets, ranging from 6-31G(d) to 6-311+G(2df,2p).[27] On this basis, full geometry optimizations have been performed for all the other energy minima and transition structures at the B3LYP/6-311G(d,p) level. Improved energy values have been obtained by 6-311+G(2df,2p) single-point computations at those geometries. Vibrational analyses were performed at the B3LYP/6-311G(d,p) level in order to confirm the nature of stationary species and to provide the harmonic frequencies needed in the computation of thermodynamic and kinetic parameters. Since the supermolecule approach can be seriously affected by the basis set superposition error (BSSE), the counterpoise method of Boys and Bernardi[28] has been used to estimate this spurious effect.

Canonical rate costants have been computed using the conventional transition state theory, whose results can be formally rewritten in terms of pseudothermodynamic functions:[29,30]

$$k(T) = \chi \frac{KT}{h}(R'T)^{-\Delta n^\dagger} \exp\frac{\Delta S^\dagger}{R} \exp\frac{-\Delta H^\dagger}{RT} = \mathrm{A}\exp\left[\frac{-E_a}{RT}\right] \quad (1)$$

In this equation K is the Boltzmann constant, h is the Planck constant, $\Delta n^\dagger$ is the variation in the number of particles in going to the transition structure (−1 for bimolecular reactions), $\Delta H^\dagger$ and $\Delta S^\dagger$ are the enthalpy and entropy changes between reactants and transition structure, R is the ideal gas constant (in units coherent with those used for $\Delta H^\dagger$ and $\Delta S^\dagger$), R' has the same meaning, but in liter inverse atmospheres (0.082), A is the so-called preexponential factor, and E_a is the activation energy. The transmission coefficient χ takes into account recrossing and tunneling effects, but a unitary value is used in the basic theory.

The electrostatic contribution to solvation energies has been evaluated by our recent implementation of the polarizable continuum model.[17,19] In this approach we solve in an essentially exact way the quantum mechanical problem of a molecule immersed in a polarizable continuum with dielectric constant ϵ (here $\epsilon = 2.42$, as recently measured for 1,1,2-trichloro-1,2,2-trifluoroethane[31]). The results are, of course, critically dependent on the shape and the dimensions of the cavity created by the solute in the solvent. Here we use the UAHF model that has been recently introduced and validated.[32] Geometry optimizations have also been performed employing analytical gradients in the presence of the solvent.[18,22]

A quantitative analysis of charge-transfer contributions can be obtained using the natural population analysis (NPA) and the Fock matrix deletion approach based on the so-called natural bond orbitals (NBO).[33] Although this procedure is not self-consistent, it leads to

(16) (a) Barone, V.; Orlandini, L. *Chem. Phys. Lett.* **1995**, *246*, 45. (b) Bottoni, A. *J. Chem. Soc., Perkin Trans. 2* **1996**, 2041. (c) Jursic, B.S. *J. Chem. Soc., Perkin Trans. 2* **1997**, 637.

(17) Cossi, M.; Barone, V.; Cammi, R.; Tomasi, J. *Chem. Phys. Lett.* **1996**, *255*, 327.

(18) Barone, V.; Cossi, M.; Tomasi, J. *J. Comput.Chem.* **1998**, *19*, 407.

(19) Miertùs, S.; Scrocco, E.; Tomasi, J. *Chem. Phys.* **1981**, *55*, 117.

(20) *Gaussian 94* (Revision D.4): M. J. Frisch, G. W. Trucks, H. B. Schlegel, P. M. W. Gill, B. G. Johnson, M. A. Robb, J. R. Cheeseman, T. A. Keith, G. A. Petersson, J. A. Montgomery, K. Raghavachari, M. A. Al-Laham, V. G. Zakrewski, J. V. Ortiz, J. B. Foresman, B. Cioslowski, B. Stefanov, A. Nanayakkara, M. Challacombe, C. Y. Peng, P. Y. Ayala, W. Chen, M. W. Wong, J. L. Andres, E. S. Replogle, R. Gomperts, R. L. Martin, D. J. Fox, J. S. Binkley, D. J. Defrees, J. Baker, J. P. Stewart, M. Head-Gordon, C. Gonzalez, J. A. Pople, Gaussian Inc., Pittsburgh, PA, 1995.

(21) Rega, N.; Cossi, M.; Barone, V. *J. Chem. Phys.* **1996**, *105*, 11060.

(22) Rega, N.; Cossi, M.; Barone, V. *J. Am. Chem. Soc.* **1997**, *119*, 12962.

(23) Viehe, H. G.; Janousek, Z.; Merényi, R.; Stella, L. *Acc. Chem. Res.* **1985**, *18*, 148.

(24) Becke, A.D. *Phys. Rev.* **1988**, *38*, 3098.

(25) Lee, C.; Yang, W.; Parr, R. G. *Phys. Rev. B* **1988**, *37*, 785.

(26) Becke, A. D. *J. Chem. Phys.* **1993**, *98*, 5648.

(27) Description of basis sets and explanation of standard levels of theory can be found in the following: Foresman, J. B.; Frisch, A. E. *Exploring Chemistry with Electronic Structure Methods*, 2nd ed.; Gaussian, Inc.: Pittsburgh, PA, 1996.

(28) Boys, S.; Bernardi, F. *Mol. Phys.* **1970**, *19*, 553.

(29) Eyring, H.; Liu, S. H.; Liu, S. M. *Basic Chemical Kinetics*; Wiley: New York, 1980.

(30) Arnaud, R.; Subra, R.; Barone, V.; Lelj, F.; Olivella, S.; Sole, A.; Russo, N. *J. Chem. Soc., Perkin Trans. 2* **1986**, 1517.

(31) We thank Prof. H. Fischer and Dr. T. Zytowski (University of Zurich) for kindly performing this measurement.

(32) Barone, V.; Cossi, M.; Tomasi, J. *J. Chem. Phys.* **1997**, *107*, 3210.

Table 1. Geometric (Å, deg) and Energetic (kJ mol^{-1}) Characteristics of the TS and the Product of CH_3 Addition to C_2H_4 Obtained by Different Basis Sets Using the B3LYP Method

	6-31G(d)	6-311G(d,p)	6-311+G(2df,2p)
R_{CC}	2.366	2.332	2.325
r_{CC}	1.355	1.355	1.353
ϕ	110.1	109.8	109.8
ΔE	18.3	22.6	25.7
BSSE	7.2	3.6	1.0
$\Delta E'$	25.5	26.2	26.7
R_{CC}	1.548	1.547	1.547
r_{CC}	1.493	1.488	1.487
ϕ	113.3	113.3	113.3
ΔE_r	−119.1	−105.2	−99.0
BSSE	11.8	5.9	1.0
$\Delta E'_r$	−107.3	−99.3	−98.0

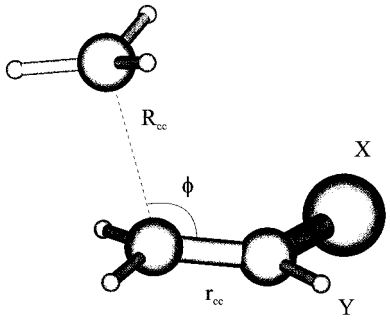

Figure 1. Definition of the key geometrical parameters in the transition stuctures for the addition of methyl radical to disubstituted alkenes $H_2C{=}CXY$.

negligible energy errors as long as the interactions that have been dropped from the Fock matrix are not strongly coupled with other interactions.[34]

3. Results and Discussion

The prototypical addition of CH_3 to ethylene has been used to select the most effective computational level. The most significant results for this system are collected in Table 1, and the geometrical parameters defining the structures of stationary points are shown in Figure 1.

Concerning geometrical parameters, nearly converged results are obtained at the 6-311G(d,p) level, whereas the 6-31G(d) basis set significantly overestimates the length of the incipient CC bond in the transition structure (TS). Energetic parameters are less sensitive to the geometry provided that a consistent level is used throughout. As a matter of fact going from 6-31G(d) to 6-311+G(2df,2p) geometries modifies the results by less than 1 kJ mol^{-1}. We think, therefore, that B3LYP/6-311G(d,p) geometries and vibrational frequencies can be confidently used for all the computations. For larger systems even 6-31G(d) geometries are probably sufficient.

The total and zero-point energies for the reactants, transition structures, and products of all the reactions considered in the present study are given in Table 2, which appears in the Supporting Information, whereas the most significant geometric and energetic parameters are given in Tables 3 and 4, respectively. Complete **Z** matrixes of all the transition structures are given in the Supporting Information.

(33) Curtiss, L. A.; Pochatko, D. J.; Reed, A. E.; Weinhold, F. *J. Chem. Phys.* **1983**, *82*, 2679.

(34) Tyrell, J.; Weinstock, R. B.; Weinhold, F. *Int. J. Quantum Chem.* **1981**, *19*, 781.

Table 3. Optimized Values of the Most Relevant Geometrical Parameters of the Transition States Related to CH_3 Addition Reactions to $H_2C{=}CXY$[c]

entry	X, Y	R_{CC} (Å)[a]	r_{CC} (Å)[b]	ϕ (deg)[a]
1	H, H	2.332 (2.246)	1.355 (0.028)	109.8 (109.1)
2	H, F	2.332 (2.246)	1.346 (0.026)	109.9 (109.9)
3	H, NH_2	2.365 (2.240)	1.360 (0.023)	109.4 (111.0)
4	H, Cl	2.368 (2.264)	1.347 (0.025)	109.5 (108.9)
5	H, CHO	2.450 (2.312)	1.355 (0.021)	108.7 (107.6)
6	H, CN	2.455 (2.313)	1.355 (0.021)	108.9 (107.5)
7	H, Me	2.333	1.357 (0.028)	109.6
8	H, OMe	2.360	1.354 (0.024)	109.5
9	Cl, Cl	2.414	1.345 (0.022)	108.4
10	Me, Cl	2.367	1.350 (0.025)	109.0
11	Me, Me	2.336	1.360 (0.027)	109.4
12	Me, OMe	2.365	1.358 (0.025)	108.4
13	Me, CN	2.454	1.358 (0.021)	108.6
14	NH_2, CHO	2.588	1.362 (0.014)	107.6
15	NH_2, CN	2.512	1.360 (0.017)	107.2

[a] UHF/6-31G(d) values in parentheses from ref 8a. [b] The values in parentheses are the differences: r_{CC}(TS) − r_{CC}(alkene). [c] The geometrical parameters are defined in Figure 1.

The same general trends observed for C_2H_4 are obtained for all the other systems. In particular the difference between 6-311G(d,p) and 6-311+G(2df,2p) energies is nearly constant both for energy barriers (∼3 kJ mol^{-1}) and reaction energies (∼8 kJ mol^{-1}). As a consequence general trends are essentially the same for both basis sets. Although both series of data are shown in some tables, we will discuss in detail in the following 6-311G(d,p) results for two reasons. From one side, this is the level selected in previous QCISD(T) computations;[8] from the other side this basis set is small enough to allow the computation of geometries, energies, and vibrational frequencies for large systems.

We have also investigated the impact of basis set superposition error (BSSE) in modifying the results. For the $CH_2{=}CH_2 + CH_3$ system, the BSSE correction is halved in going from 6-31G(d) to 6-311G(d,p) basis sets, and becomes essentially negligible (∼1 kJ mol^{-1}) at the 6-311+G(2df,2p) level. After correction for BSSE, the energy barriers obtained by different basis sets become very similar to each other. As expected, BSSEs are significantly larger for reaction energies ΔE_r than for energy barriers, $\Delta E^{\dagger}$; however, also in this case, the results obtained by different basis sets become quite similar after removal of BSSE.

From another point of view, one of the most serious drawbacks of unrestricted computations of open-shell species is that the resulting wave function is not an eigenstate of the S^2 operator. Although the DF approach does not use, in principle, any well-defined wave function, the spin density is evaluated using a reference set of KS orbitals. Under such circumstances the expectation value of S^2 computed for these orbitals should provide a reliable estimate. It is then remarkable that spin contamination is very low by the UKS approach both for product radicals ($0.75 < S^2 < 0.76$) and for transition structures ($0.75 < S^2 < 0.78$), whereas much higher spin contaminations are obtained by the UHF approach especially for transition structures (S^2 values up to 1.1).[8]

A last point of interest concerns the comparison between rate constants (actually ln K) and activation energies (E_a) or potential energy barriers ($\Delta E^{\dagger}$). As a matter of fact, a good correlation between the first two quantities should validate the derivation of activation energies from experimental rate constants using a constant preexponential factor for all the methyl additions.[7] At the same time, a good correlation between ln K and $\Delta E^{\dagger}$ would

Table 4. Energetic Characteristics (kJ mol^{-1}), Imaginary Frequencies at the TS (cm^{-1}), Activation Entropies (J mol^{-1} K^{-1}), and Natural Logarithms of Rate Constants (L^2 mol^{-1} s^{-1}) for CH_3 Additions to Substitued Alkenes Obtained by UB3LYP and UQCISD(T) Methods

	$\Delta E^{\dagger}$			$i\omega^{\dagger}$	ΔZPE	$\Delta S^{\dagger}$	ln K	ΔE_r		
X, Y	UB3LYP[a]	UB3LYP[b]	UQCISD(T)[c]	UB3LYP[a]	UB3LYP[a]	UB3LYP[a]	UB3LYP[a]	UB3LYP[a]	UB3LYP[b]	UQCISD(T)[c]
H, H	22.6 (26.2)	25.9	27.2	400	9.4	−117.6	7.54	−105.2 (−99.3)	−99.0	−112.6
H, F	22.7	26.0	28.3	414	8.7	−128.8	6.11	−109.6	−102.5	−117.1
H, NH_2	19.2 (23.6)	22.8	23.9	387	8.7	−126.5	7.52	−113.4 (−107.1)	−105.3	−123.3
H, Cl	17.7	21.0	21.0	375	8.5	−127.3	8.29	−119.3	−113.0	−128.1
H, CHO	10.4	13.1	18.1	289	8.3	−127.8	11.21	−139.1	−133.3	−141.1
H, CN	9.2 (12.1)	12.0	15.0	288	8.1	−125.1	12.05	−141.5 (−136.7)	−135.3	−147.5
H, Me	22.8	26.4	25.8	403	8.4	−127.3	6.28	−104.3	−97.2	−113.2
H, OMe	20.1	23.7		389	8.7	−106.2	8.89	−117.2	−109.1	
Cl, Cl	12.8	16.1		339	7.9	−119.0	10.47	−136.9	−129.9	
Me, Cl	18.0	21.5		378	7.8	−125.6	8.38	−118.9	−111.8	
Me, Me	22.3	26.1		398	8.0	−121.1	7.26	−103.4	−95.8	
Me, OMe	19.7	23.1		394	7.7	−125.6	7.74	−118.1	−110.1	
Me, CN	10.7	13.6		295	7.5	−124.1	11.61	−145.1	−138.7	
NH_2, CHO	7.6 (11.4)	10.2		247	6.2	−115.8	14.10	−181.7 (−175.4)	−176.0	
NH_2, CN	8.8	11.7		294	7.2	−120.5	12.82	−162.0	−156.4	

[a] 6-311G(d,p) basis set. In parentheses are given values including BSSE correction. [b] 6-311+G(2df,2p) basis set. [c] 6-311G(d,p) basis set from ref 8.

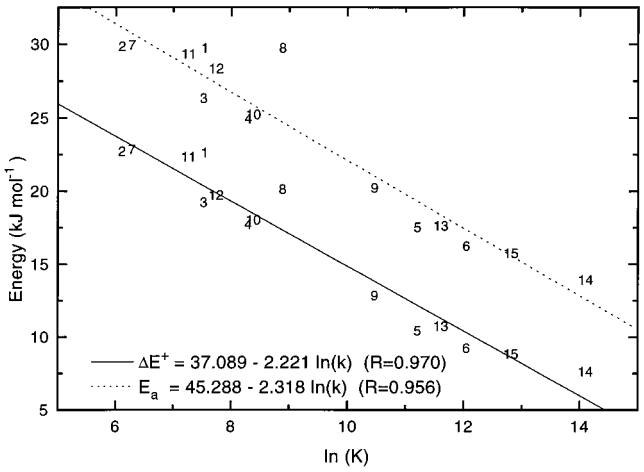

Figure 2. Correlation between rate constants (ln K), activation energies (E_a), and potential energy barriers ($\Delta E^{\dagger}$) computed at the UB3LYP/6-311G(d,p) level for the addition of methyl radical to substituted alkenes $H_2C{=}CXY$.

allow one to avoid the expensive calculation of vibrational frequencies (ω_i) needed for the evaluation of activation energies:

$$E_a = \Delta E^{\dagger} + \Delta(\mathrm{ZPE}) + (1 - 3\Delta n^{\dagger})RT + \Delta\{\sum h\omega_i/[\exp(h\omega_i/KT) - 1]\} \quad (2)$$

Figure 2 shows that substituent effects modify the reactivity of alkenes essentially due to potential energy effects, non potential energy terms (zero-point energy (ZPE), entropy) playing only a minor role. We point out, however, that from a quantitative point of view, activation entropies cannot be considered strictly constant (see Table 4).

Two other aspects must be mentioned concerning the computation of accurate reaction rates, namely, tunneling[35,36] and variational location of the transition structure.[37]

A rough estimate of tunneling effects is provided by the Wigner expression which gives a temperature-dependent transmission coefficient in terms of the single imaginary frequency ($\omega^{\dagger}$) of the transition structure:

$$\chi(T) = 1 - [ih\omega^{\dagger}/RT]^2/24 \quad (3)$$

Table 4 shows that for all the reactions considered in the present study 247 cm^{-1} < $i\omega^{\dagger}$ < 414 cm^{-1}, which leads to 1.06 < χ(298 K) < 1.17. Thus, even in the worst case, tunneling lowers the effective activation energy by (ln 1.17)/$RT \approx$ 1 kJ mol^{-1}, which is well within the bar of other errors in our approach and of the experimental incertitude. Of course, the effect of tunneling could become more significant at lower temperatures, and computation of reliable rate constants in these conditions surely requires more refined models.[35,36]

The role of a variational location of the transition structure has been investigated tracing the intrinsic reaction coordinate (IRC) for two representative reactions, namely, the prototypical addition to ethylene and that to cyanoethylene, which has a particularly low energy barrier. The corresponding curves are shown in Figure 3.

Evaluation of ZPEs and free energies for points near the conventional TS[37] shows that the locations of conventional and variational transition structures are very close in both cases. Although these and other aspects (e.g., curvature of the reaction path and proper treatment of hindered rotation of the methyl group[35,36]) could slightly alter the numerical results, we think that in the present context general trends of reaction rates are closely reproduced by the correspondidng energy barriers.

3.1. Comparison between B3LYP/6-311G(d,p) and QCISD-(T)/6-311G(d,p) Calculations. As a result of their assessment work, Radom and Wong[8a] have selected the UQCISD(T)/6-311G(d,p)//HF/6-31G(d) level of theory for an accurate description of energy barriers.

Concerning the transition structures (see Table 3), the B3LYP method predicts earlier transition states than UHF/6-31G(d) calculations. This difference cannot be attributed to a basis set effect since increasing the basis set decreases the bond length of the incipient C−C bond (R_{CC}) both at the HF[8a] and at the B3LYP[16a] levels. Correlated geometries[9a] are characterized by longer R_{CC} intermolecular distances (for example, the C−C bond increases in going from UHF to UQCISD(T) by 0.035 Å). As expected, the alkene bond length (r_{CC}) and R_{CC} show opposite variations (see Table 3), earlier TSs being characterized by lower substrate deformations. The effect of substituents on the angle of attack ϕ of the methyl radical is small, both UHF and

(35) (a) Truhlar, D. G.; Garrett, B. C. *Annu. Rev. Phys. Chem.* **1984**, *35*, 159. (b) Tucker, S.; Truhlar, D. G. In *New Theoretical Concepts for Understanding Organic Reactions*; Bertran, J., Csizmadia, I., Eds.; Kluwer: Dordrecht, 1989; p 291. (c) Truhlar, D. G. *J. Chem. Soc., Faraday Trans.* **1994**, *90*, 1740.

(36) Minichino, C.; Barone, V. *J. Chem. Phys.* **1994**, *100*, 3717. (b) Barone, V.; Minichino, C. *Theochem* **1995**, *330*, 365.

(37) Truhlar, D. G.; Garrett, B. C. *Acc. Chem. Res.* **1980**, *13*, 440.

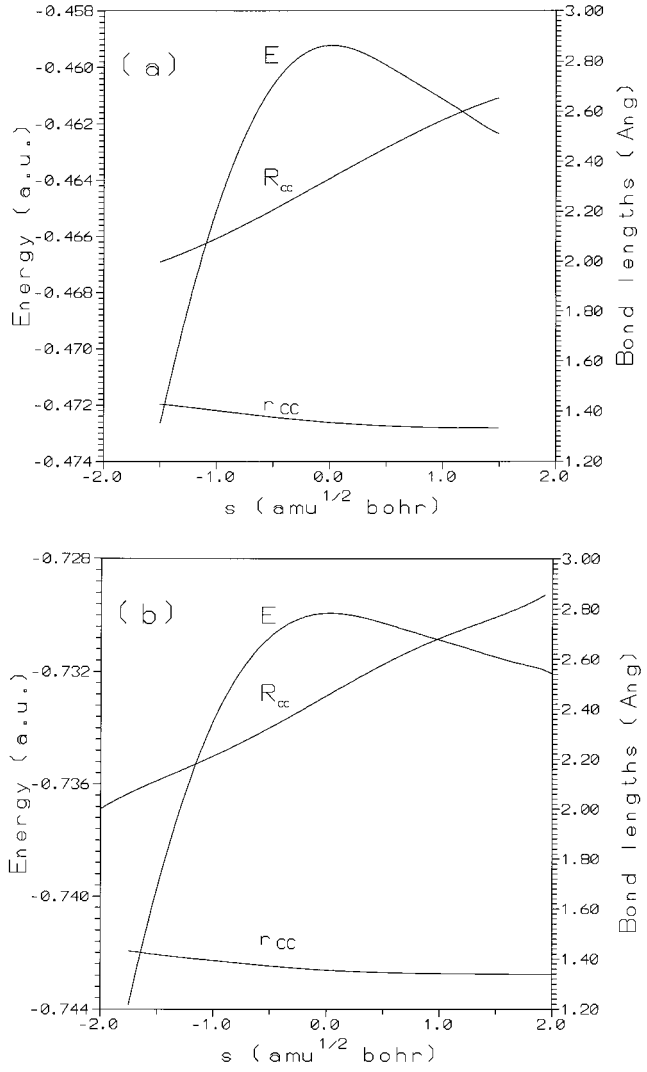

Figure 3. Potential energy and C−C distances as a function of the intrinsic reaction coordinate for the addition of methyl radical to ethylene (a) and cyanoethylene (b). The energy axes are scaled by 118 and 210 au in panels (a) and (b), respectively.

UB3LYP methods predicting a slight decrease of ϕ with the earliness of the transition state.

As shown in Figure 4, an excellent correlation ($R = 0.992$) is found between the length of the incipient CC bond at the TS and the reaction enthalpy, whose origin has already been discussed by Radom et al.[8b] This trend allows a remarkable guess of the transition structures for different alkenes using only data already available for reactants and products.

It would seem questionable to compare B3LYP energetics with QCISD(T)/UHF values, because the structures employed in the latter approach correspond to tighter TSs. Thus, it is not too surprising that B3LYP energy barriers are systematically lower than QCISD(T) ones by 2−5 kJ mol^{-1} and B3LYP reaction energies systematically lower by 3−7 kJ mol^{-1}. The central concern of this study is, however, the role of substituent effects in modifying the reactivity. From this point of view, several studies[8,16a,38] have shown that general trends are only marginally affected by different choices of the method used for geometry optimizations. It is, therefore, significant that B3LYP and QCISD(T)/UHF potential energy barriers show a very good

(38) (a) Barone, V.; Arnaud, R., *J. Chem. Phys.* **1997**, *106*, 8727. (b) Arnaud, R.; Vetere, V.; Barone, V. Manuscript in preparation.

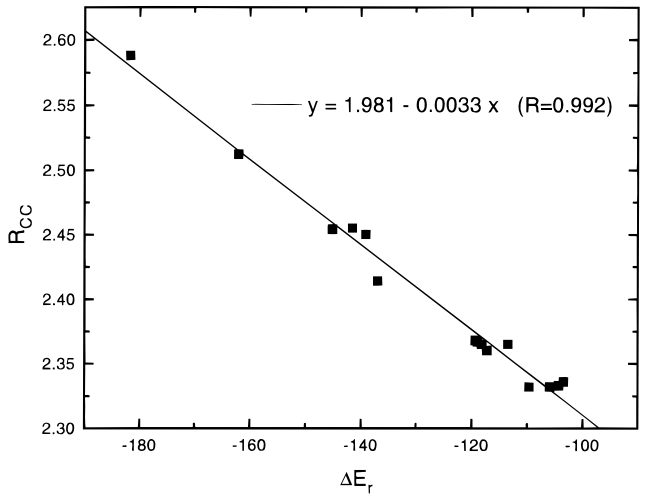

Figure 4. Correlation between C−C bond lengths in the transition structures (R_{CC}) and reaction enthalpies computed at the UB3LYP/6-311G(d,p) level for the addition of methyl radical to substituted alkenes $H_2C{=}CXY$.

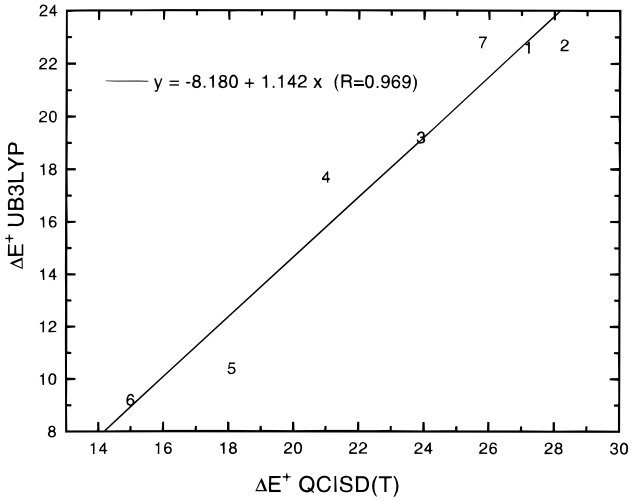

Figure 5. Correlation between energy barriers for the addition of methyl radical to substituted alkenes $H_2C{=}CHX$ calculated at the UB3LYP/6-311G(d,p) and UQCISD(T)/6-311G(d,p) levels.

correlation ($R = 0.969$; see Figure 5) and the same applies to reaction energies ($R = 0.970$).

From these results we can conclude that two quite different quantum mechanical methods provide very close reactivity orders for methyl additions to substituted alkenes. We have also checked that the B3LYP model reproduces the trends of electron affinities computed at the G2(MP2) level[27] in ref 8. The very good correlation between the two sets of data (EA(B3LYP) = −0.003 + 1.151 EA(G2(MP2), $R = 0.999$) increases our confidence in the B3LYP computational model.

3.2. Comparison between B3LYP Computations and Experimental Data. Table 5 collects the activation energies (E_a) and the reaction enthalpies (ΔH_r) at 298 K in the gas phase and in solution for the addition of methyl radical to 11 substituted alkenes selected among those considered by Fischer and co-workers in their experimental studies.[7a,39] The calculated electron affinities of these alkenes and the values of E_a and ΔH_r corresponding to the addition of CH_3 to alkenes **14** and **15** which lead to products stabilized by a captodative effect are also given in Table 5.

(39) Wu, J. Q.; Fischer, H. *Int. J. Chem. Kinet*. **1995**, *27*, 167.

Table 5. Comparison between UB3LYP/6-311G(d,p) and Experimental Activation Energies E_a (kJ mol^{-1}), Reaction Enthalpies ΔH_r (kJ mol^{-1}), and Electron Affinities EA (eV)

	E_a (298 K)[a]			ΔH_r (298 K)			EA(alkene)	
	UB3LYP[b]	UB3LYP[c]	exp[d]	UB3LYP[b]	UB3LYP[c]	exp[d]	UB3LYP[b]	exp[e]
H, H	29.7	30.0	28.2	−91.3	−91.0	−98	−2.14	−1.78
H, Cl	24.9	25.5	23.9	−102.6	−102.0	−106	*g*	−1.28
H, CHO	17.5	17.0	15.0	−122.0	−122.5	−118	0.00	0.03
H, CN	16.2	16.4	15.4	−127.4	−126.9	−139	−0.24	−0.21
H, Me	29.9	30.4	27.7	−88.9	−88.6	−104	−2.08	−1.99
H, OMe	29.7	30.2	24.8	−96.9	−95.7	−106	−2.02	−2.24
Cl, Cl	20.2	20.4	17.9	−117.7	−117.1	−119	*g*	−0.76
Me, Cl	25.2	24.8	22.5	−101.3	−101.1	−96	*g*	−1.44
Me, Me	29.3	29.7	26.0	−87.6	−87.2	−100	−2.19	−2.19
Me, OMe[f]	28.3	28.6	25.1	−100.4	−99.4	−109	−2.14	−2.48
Me, CN	17.6	18.5	16.0	−127.6	−127.1	−127	−0.33	−0.17
NH_2, CHO	13.9	12.8		−162.0	−167.2		−0.31	
NH_2, CN	15.7	15.7		−145.1	−150.0		−0.53	

[a] $E_a = \Delta E^{\dagger} + \Delta ZPE^{\dagger}$ + therm corr + RT (2.47 kJ mol^{-1} at 298 K). [b] For $H_2C{=}CHF$ and $H_2C{=}CHNH_2$, E_a = 29.8, 26.3 kJ mol^{-1}; ΔH_r = −92.7, −95.7 kJ mol^{-1}; EA = −1.83, −2.27 eV, respectively. [c] Including solvent effects by PCM. [d] From ref 7a. [e] From ref 33. [f] Measured for Y = OEt. [g] Geometry optimization of the radical anion leads to Cl dissociation.

The solvent effect on the alkenes and TS geometries is weak (for example, R_{CC} values without and with solvent are, respectively, 2.332 and 2.331 Å for **1**, 2.450 and 2.460 Å for **5**, and 2.455 and 2.458 Å for **6**). Our calculations indicate that geometry reoptimization in the presence of the solvent does not modify the energetic values obtained with geometries optimized in vacuo, and we further assume that non potential energy effects (ZPE, thermal corrections) are not modified by the presence of the solvent. On this basis, E_a and ΔH_r values in solution are simply obtained by adding the appropriate differences of solvation energies (obtained by single-point PCM computations) to the values computed for the reactions in vacuo. The solvent effect on reaction enthalpies is marginal (<1 kJ mol^{-1}) except for species involving a captodative effect (**14**, **15**) where it stabilizes the product by about 5 kJ mol^{-1}. The effect on activation energies is also quite low, the largest difference (1.1 kJ mol^{-1}) being calculated for **14**. In any case, the trends obtained *in vacuo* are retained also for reactions in solution. This is not surprising in view of the low dielectric constant of the solvent and of the lack of strong charge separation effects in radical reactions.

As a general rule calculated activation energies are quite close to their experimental counterparts, the largest deviation (−5.4 kJ mol^{-1}) being obtained for **8**. As mentioned above, the good correlation obtained when using values computed in vacuo (R = 0.980, Figure 6, top) is only slightly improved by including solvent effects (R = 0.981, Figure 6, bottom). All these results point out that the B3LYP method quantitatively reproduces substituent effects on activation barriers and that the discrepancy between experimental[7] and quantum mechanical[8] trends is not due to solvent and/or non potential energy effects.

Let us now discuss reaction enthalpies. As a first point, we recall that "experimental" ΔH_r values (see Table 5) are in fact estimated from formation enthalpies and bond dissociation energies (BDE).[39] Close examination of the values given in Table 5 reveals some discrepancies between calculated and estimated ΔH_r values, and Figure 7 shows that these two quantities do not correlate very well (R = 0.887). In our opinion, this disagreement originates essentially from the evaluation of BDEs of CH_3CH_2CXY species and not from a failure of the B3LYP method which reproduces well QCISD-(T) results (see section 3.1).

Methyl additions to species **14** and **15** are more exothermic than to species **5** and **6** by 40.0 and 17.7 kJ mol^{-1}, respectively. This trend is in agreement with previous theoretical work on carbon-centered radicals,[40] showing that the captodative effect is larger for the combination of nitrogen and carbonyl geminal substitution. In this connection we recall that it is extremely

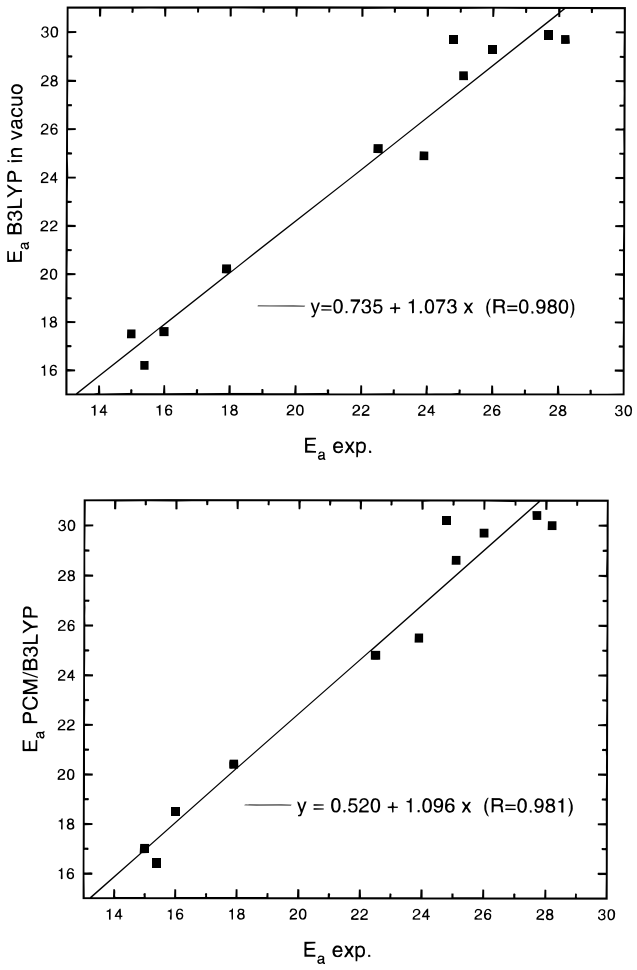

Figure 6. Correlation between activation energies E_a for the methyl addition to substituted alkenes $H_2C{=}CXY$ calculated at the UB3LYP/6-311G(d,p) level and experimental values: (top) E_a in vacuo; (bottom) E_a in solution.

(40) (a) Pasto, D. J. *J. Am. Chem. Soc.* **1988**, *110*, 8164. (b) Leroy, G.; Sana, M.; Wilante, C. *J. Mol. Struct.: THEOCHEM* **1991**, *234*, 303. (c) Espinosa-Garcia, J.; Olivares del Valle, F. J.; Leroy, G.; Sana, M. *J. Mol. Struct.: THEOCHEM* **1992**, *258*, 315. (d) Davidson, E. R.; Chakravorty, S.; Gajewski, J. J. *New J. Chem.* **1997**, *21*, 533.

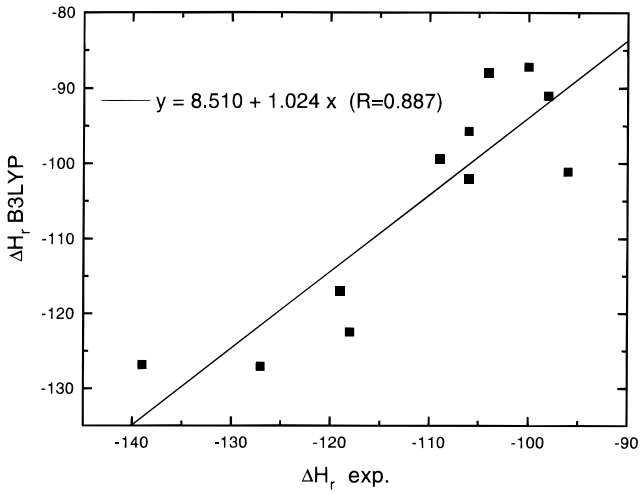

Figure 7. Correlation between reaction enthalpies for methyl adddition to substituted alkenes $H_2C{=}CHX$ calculated at the UB3LYP/6-311G-(d,p) level and "experimental" values.

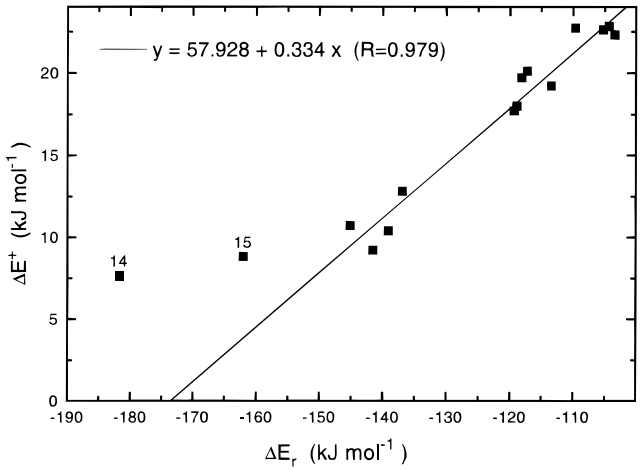

Figure 8. Correlation between potential energy barriers and reaction energies computed at the UB3LYP/6-311G(d,p) level for methyl addition to substituted alkenes $H_2C{=}CXY$.

difficult to compute accurate formation enthalpies of free radicals by conventional quantum mechanical methods.[41,42] Thus, the good performances of the B3LYP approach are particularly significant and will be further investigated in a forthcoming systematic study.

3.3. Factors Controlling the Methyl Reactivity. In this paragraph we analyze, on the grounds of B3LYP results, the role of thermodynamic and polar contributions in determining the reactivity of methyl radical toward substituted alkenes.

As mentioned in the Introduction, a good correlation between activation energies and reaction enthalpies is diagnostic of a dominant role of enthalpic contributions. Here we prefer to employ in vacuo potential energy barriers and reaction energies (see Figure 8), which do not include zero-point, entropic, and solvent contributions.

The good correlation obtained neglecting species **14** and **15** ($R = 0.979$) confirms that, as already pointed out by Radom et al.,[8a] the reaction exothermicity is a key factor in determining the reactivity. The slope of the correlation line (0.35) is slightly smaller than that obtained by these authors (0.41); this result is

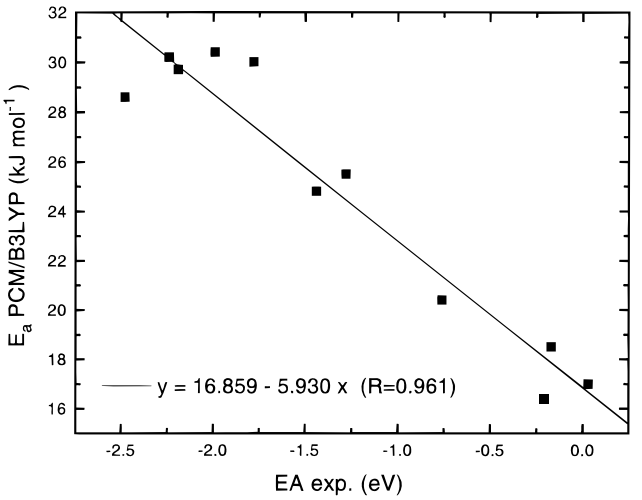

Figure 9. Correlation between PCM/UB3LYP activation energies and experimental electron affinities for the addition of methyl radical to substituted alkenes $H_2C{=}CXY$.

in line with the accepted interpretation of the slope of the correlation line[43] insofar as B3LYP TSs occur earlier along the reaction coordinate (see section 3.1). We recall that B3LYP and QCISD(T) calculations provide comparable ΔH_r values, which, in some cases, deviate considerably from the values estimated from formation enthalpies and bond dissociation energies.[7] The inaccuracy of some of the estimated values could well explain the poor correlation between activation energies and reaction enthalpies found by Fischer et al. ($R = 0.668$).

On the other hand, if polar interactions play a dominant role, nucleophilic behavior of the methyl radical would lead to a good correlation between activation energies and electron affinities of the alkenes.[7] While Figure 9 shows that this correlation is remarkably good ($R = 0.961$), the nucleophilic character of the methyl radical is not unambiguously proven because a direct correlation exists between ΔH_r and EA ($R = 0.911$) for the series of alkenes considered till now.

A possible way to overcome this ambiguity is offered by 1,1-disubstituted alkenes which give, upon methyl addition, radical adducts stabilized by a captodative effect. As shown by the ΔH_r and EA values calculated for **14** and **15** (see Table 4) in this case the correlation between reaction enthalpy and alkene electron affinity is broken. With respect to **5** and **6**, the activation barrier is lowered by 3.6 and 0.5 kJ mol^{-1}, respectively, while the reaction exothermicity increases by 40.0 and 17.7 kJ mol^{-1} and the electron affinity decreases by 0.31 and 0.29 eV, respectively. This trend suggests that reaction enthalpy is the dominating factor, but **14** and **15** lie above the correlation line of all the other substituted alkenes, and this might be attributed to a lower polar stabilization. Actually Figure 9 shows that a linear correlation between reaction enthalpies and energy barriers would lead, for strongly exothermic reactions, to negative activation energies. Although this is not totally surprising for radical addition reactions,[41] complete computations (Table 4) indicate that positive, albeit small, energy barriers are always connected to methyl additions. This question can be settled, in our opinion, by comparison with the trend obtained for a genuine nucleophilic radical like hydroxymethyl, CH_2-OH.[8b,39] Then, for the hydroxymethyl addition, we can expect a much lower decrease of the energy barrier in going from $H_2C{=}CH(CHO)$ to $H_2C{=}C(CHO)(NH_2)$ or even an increase of the latter if the polar contribution predominates. The results

(41) Villa, J.; Gonzalez-Lafont, A.; Lluch, J. M.; Corchado, J. C.; Espinosa-Garcia, J. *J. Chem. Phys.* **1997**, *107*, 7266.

(42) Mayer, P. M.; Parkinson, C. J.; Smith, D. M.; Radom, L. *J. Chem. Phys.* **1998**, *108*, 604.

(43) Jencks, W. P. *Chem. Rev.* **1985**, *85*, 5111 and references therein.

Table 6. Thermodynamic and Kinetic Parameters (kJ mol^{-1}) for CH_2OH and CH_3 Addition to $H_2C{=}CHCHO$ and $H_2C{=}C(NH_2)CHO$ Computed at the UB3LYP/6-311G(d,p) Level

	CH_2OH addition to		CH_3 addition to	
	$H_2C{=}CHCHO$	$H_2C{=}C(NH_2)CHO$	$H_2C{=}CHCHO$	$H_2C{=}C(NH_2)CHO$
$\Delta E^\dagger$	3.8	6.7	10.4	7.6
$\Delta H^\dagger$ (0 K)	10.1	11.3	18.7	13.8
ΔE_r	−112.3	−157.1	−139.1	−181.7
ΔH_r (0 K)	−95.7	−142.4	−116.2	−156.9

Table 7. Amount of Electron Transfer ΔQ (electron units) and Charge-Transfer Energy E_{CT} (kJ mol^{-1}) Related to Addition Reactions to $H_2C{=}CXY$

entry	X, Y	ΔQ[a]	E_{CT}(R → S) (1)	E_{CT}(S → R) (2)	(1)/(2)
			CH_3 Addition		
1	H, H	−0.005	−114.2	−165.3	0.69
2	H, F	−0.018	−107.1	−192.5	0.56
3	H, NH_2	−0.069	−95.0	−200.0	0.47
4	H, Cl	0.001	−112.1	−147.7	0.76
5	H, CHO	0.039	−84.5	−101.7	0.83
6	H, CN	0.039	−93.7	113.0	0.83
7	H, Me	−0.022	−114.2	−162.8	0.70
8	H, OMe	−0.048	−96.7	−193.3	0.50
9	Cl, Cl	0.005	−97.5	−130.5	0.75
10	Me, Cl	−0.008	−103.8	−148.5	0.70
11	Me, Me	−0.033	−105.8	−164.0	0.64
13	Me, CN	0.025	−86.2	−113.4	0.76
14	NH_2, CHO	−0.017	−51.0	−106.5	0.48
15	NH_2, CN	−0.009	−67.7	−126.0	0.54
			CH_2OH Addition		
5	H, CHO	0.123	−147.1	−97.5	1.51
14	NH_2, CHO	0.061	−93.6	−84.4	1.11

[a] NPA population analysis; a positive value indicates electron transfer from the radical R to the alkene S.

obtained for these two systems are compared in Table 6 with the corresponding values for methyl additions.

From a quantitative point of view, the $\Delta H^\dagger$ for addition of the hydroxymethyl radical to $H_2C{=}CHCHO$ obtained at the B3LYP/6-311G(d,p) level (10.1 kJ mol^{-1}) is significantly lower than the corresponding QCISD/6-311G(d,p) value (18.3 kJ mol^{-1}).[8b] However, the B3LYP result, when corrected to 298 K using our computed vibrational frequencies and adding the *RT* term, becomes 10.4 kJ mol^{-1}, very close to the experimental activation energy[39] of 12 kJ mol^{-1}. Furthermore, inclusion of ZPE corrections and of solvent effects does not modify the trend given by $\Delta E^\dagger$ values computed in vacuo.

As expected, for CH_2OH the $\Delta E^\dagger$ of **5** is lower than that of **14**, whereas just the opposite occurs for CH_3. Thus, polar effects dominate for the strongly nucleophilic hydroxymethyl radical, whereas enthalpic effects are more important for methyl. This does not mean, in our opinion, that polar effects are not important in radical additions to unsaturated bonds, but, rather, that the methyl radical is not particularly nucleophilic. This hypothesis can be further checked by a population analysis or by computing the charge-transfer energies E_{CT} in the transition stuctures: for nucleophilic radicals one expects a net electron transfer from the radical R to the substrate S and the predominance of the E_{CT}(R → S) term in comparison with the E_{CT}(S → R) term. As shown in Table 7, both conditions are fulfilled by the hydroxymethyl radical, whereas CH_3 shows a more erratic behavior. In particular, a weak electron transfer from the substrate to CH_3 (i.e., an electrophilic character of the radical) is obtained except in the case of alkenes **5**, **6**, and **13**.

An even stronger indication is offered by the ratio E_{CT}(R → S)/E_{CT}(S → R) which, in the case of CH_3, is lower than 1 for the entire set of alkenes, the maximum value (0.83) being obtained for the electron-deficient alkenes **5** and **6**: using this criterion, CH_3 always behaves as an electrophile. On the contrary, in the case of the addition of the nucleophilic hydroxymethyl radical, the ratio is always larger than 1, in agreement with the nucleophilic character of the radical.

4. Concluding Remarks

In the present work we have explored the role of different factors in determining the reactivity of methyl radical toward substituted alkenes by means of a comprehensive quantum-mechanical approach. From the ensemble of our results we can draw the following conclusions:

(1) UB3LYP/6-311G(d,p) calculations reproduce well the variations both of activation barriers and of reaction enthalpies for the addition of methyl radical to monosubstituted alkenes given by the most sophisticated post-HF methods.

(2) A satisfactory correlation is found between B3LYP and experimental activation energies for the methyl addition to 11 monosubstituted or 1,1-disubstituted alkenes. These results suggest that the B3LYP functional can be confidently used to investigate substituent effects in this class of reactions.

(3) Our calculations show that solvents with low dielectric constants have little effect on barrier heights and enthalpies in this class of reactions. Also non potential energy effects (ZPE, entropy) do not alter the trends provided by electronic energies alone.

(4) The separation between enthalpic and polar contributions to the reactivity of methyl radical toward alkenes is improved by studying its addition to geminal donor−acceptor-substituted alkenes, which leads to products stabilized by captodative effects. In this way, our results bring over new evidence that the reactivity of methyl radical toward alkenes is essentially governed by enthalpic effects.

Acknowledgment. This work was generously supported by the French (CNRS) and Italian (CNR) National Research Councils. A generous allocation of computer time by the CNUSC is also gratefully acknowledged.

Supporting Information Available: Table 2 and **Z** matrixes for all the transition structures (17 pages, print/PDF). See any current masthead page for ordering information and Web access instructions.

JA973896P